Highly Sensitive Fiber-Optic Sensor for Dynamic Pressure Measurements

Wojtek J. Bock, *Senior Member, IEEE*, Magdalena S. Nawrocka, and Waclaw Urbanczyk

***Abstract*—A new type of fiber-optic pressure sensor based on a specially developed side-hole fiber is presented. It allows for unambiguous and fast phase-shift measurements in the range from $-\pi/2$ to $+\pi/2$ with a sampling rate of 5 kHz and resolution of about 1% of full scale ($2 \cdot 10^{-3}$ atm).**

***Index Terms*—Dynamic measurements, fiber-optic sensor.**

I. INTRODUCTION

THERE are many different sensing principles used in fiber-sensors [1]–[3]. It has been already reported in the literature that highly birefringent (HB) fibers are a good tool for measuring slowly changing pressure, temperature, and elongation [4]–[6]. HB fibers have also been tested in measurements of dynamic pressure changes [7]. The main drawback of solutions applied so far is temperature compensation schema, in which sensing and compensating fibers are located in different compartments of the sensor housing. The pressure has access only to the sensing fiber, while the compensating one serves as a reference. Such construction is not best suited for dynamic pressure measurements. This is because fast compressions and decompressions are always associated with temperature changes. If the sensing and compensating fibers are located at different places, the temperature gradients arise, causing the sensor false reading. Therefore, for good temperature compensation in dynamic measurements, the sensing and compensating fibers must be located in the same place. This requirement is fulfilled in the proposed sensor construction. It was made possible by application of a white-light detection schema and a specially developed side-hole fiber with negative and very high sensitivity to hydrostatic pressure. Furthermore, in comparison to already presented solutions, our system has much better resolution of pressure measurements, equal to $2 \cdot 10^{-3}$ atm.

II. FIBER USED IN SENSOR CONSTRUCTION

The active part and the leadings of the proposed sensor are made of HB fibers operating in a single mode regime. In this case, two orthogonally polarized modes LP_{01}^X and LP_{01}^Y propagate in the fiber with different propagation constants β_X and β_Y, respectively. One of the parameters characterizing the HB fiber is the phase modal birefringence Δn defined in the following way:

$$\Delta n = \frac{\lambda}{2\pi}(\beta_X - \beta_Y) \tag{1}$$

where λ is wavelength. External parameters acting on such elements cause change in the initial phase shift between orthogonally polarized modes. This phase shift is measured using the interferometric method. A parameter characterizing the fiber response to a given measurand is sensitivity, which is defined in the following way:

$$K_X = \frac{\Delta\varphi}{\Delta X L} \tag{2}$$

where $\Delta\varphi$ is the phase shift induced by the measurand change by ΔX, and L is the length of the fiber exposed to the measurand. Note that K_X is associated with the change of modal birefringence induced by the parameter X, and can be also expressed as

$$K_X = \frac{2\pi}{\lambda}\frac{\partial \Delta n}{\partial X}. \tag{3}$$

The main difficulty associated with applying HB fibers as active elements of fiber-optic sensors is associated with the fact that they are sensitive to many physical parameters such as temperature, hydrostatic pressure, lateral and axial stress, etc. Therefore, the overall phase response of the sensor may be induced simultaneously by many physical parameters. In case of hydrostatic pressure measurements, the sensing part of the fiber can be easily isolated from any axial or lateral stress by proper design of the sensor housing. To reduce temperature drift the sensor is optically compensated for temperature. To make the compensation most effective, we used as an active element a specially developed HB fiber (side-hole fiber), which shows high sensitivity to pressure $K_{SH}^P = -100$ rad/MPa m and at the same time moderate sensitivity to temperature $K_{SH}^T = -0.5$ rad/K m. This fiber was developed by Fiber Optic Technology Group, UMCS University, Lublin, Poland [8], [9]. High sensitivity to pressure was achieved by introducing into the fiber cladding two air channels parallel to the elliptical core. The cross section of the fiber is shown in Fig. 1. The elliptical core assures high modal birefringence of the order of 10^{-4} and, therefore, prevents energy coupling between polarization modes. It is worth mentioning that in the side-hole fiber we used the ratio of sensitivities $K_{SH}^P/K_{SH}^T = 200$ K/MPa while in other commercially available fibers K_{SH}^P/K_{SH}^T is lower than 2 K/MPa. It makes this fiber especially suitable for low-pressure sensing.

Another important feature of this fiber is negative sign of pressure sensitivity, which is unlike other HB fibers. Negative

Manuscript received May 4, 2000; revised June 22, 2001. This work was supported by the Polish Committee for Scientific Research under Grant 8T10C 020 18 and by the Natural Sciences and Engineering Research Council of Canada.

W. J. Bock is with the Laboratoire d'optoélectronique, Département d'informatique, Université du Québec, Hull, PQ J8X 3X7, Canada.

M. S. Nawrocka and W. Urbanczyk are with the Institute of Physics, Wroclaw University of Technology, 50-370 Wroclaw, Poland.

Publisher Item Identifier S 0018-9456(01)08754-X.

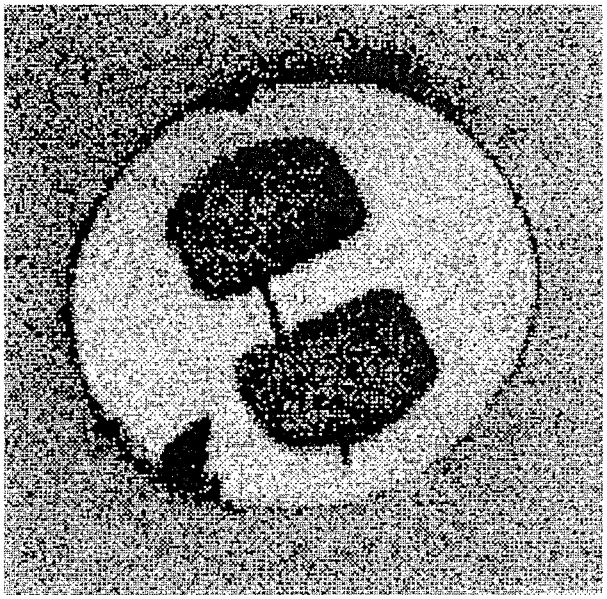

Fig. 1. Cross section of the side-hole fiber used as a sensing element.

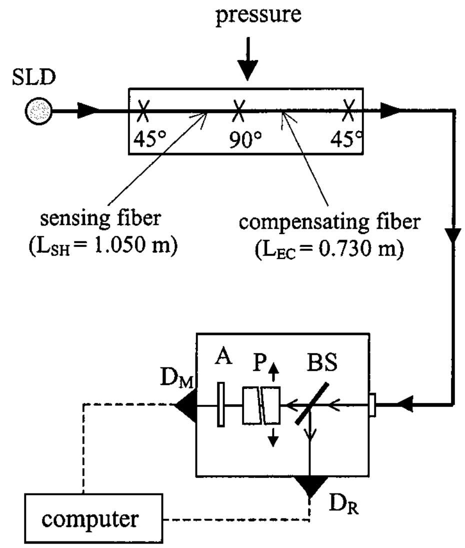

Fig. 2. Scheme of the fiber-optic pressure sensor: SLD—superluminescent diode, BS—beam splitter, R—quartz retardation plate composed of two wedges, A—analyzer, D_M—signal detector, D_R—reference detector.

sign indicates that birefringence decreases with increasing pressure. This unique feature of the side-hole fiber allowed for application of a new temperature compensation schema, in which pressure has access to both the sensing and the compensating element. The pressure and temperature sensitivities of this fiber were measured using the low coherence interferometric method described in [10], which allows also for determining the sign of sensitivity.

III. Principle of Sensor Operation

The proposed sensor is based on a coherency addressing configuration [1]. Such a sensor is usually composed of sensing and decoding interferometers with matched optical path delays. In our case, the sensing interferometer is based on HB fibers, while a quartz crystalline plate with an analyzer is used as a decoding element (see Fig. 2). As a light source in our system, a superluminescent diode pigtailed with 3M polarizing fiber is used ($\lambda_0 = 830$ nm, $\Delta\lambda = 25$ nm, $P = 0.2$ mW). Linearly polarized light from the polarizing fiber is coupled by a polarization maintaining connector into one mode of the linking fiber (Corning PMF-38). The linking fiber and the active part of the sensor are spliced to each other with rotation of their polarization axes by 45°. Therefore, two polarization modes are excited in the sensor's active part, which is composed of sensing (side-hole) and compensating (elliptical core) fiber spliced with rotation of their polarization axes by 90°. The sensitivity of the elliptical core fiber to pressure and temperature is equal to $K_{EC}^P = +0.5$ rad/MPa m and $K_{EC}^T = -0.7$ rad/K m, respectively.

When these two elements are exposed to simultaneous changes in pressure and temperature, the phase shift induced at the sensor output can be expressed by the following equation:

$$\Delta\phi_S = (K_{EC}^P L_{EC} - K_{SH}^P L_{SH})\Delta p + (K_{EC}^T L_{EC} - K_{SH}^T L_{SH})\Delta T + \Delta\phi_0 \quad (4)$$

where L_{EC} and L_{SH} are lengths of the elliptical core and the side-hole fiber, and $\Delta\phi_0$ is the phase shift associated with the length imbalance of the sensor elements at atmospheric pressure and room temperature.

In order to make the sensor totally insensitive to temperature changes, the following condition must be fulfilled:

$$K_{EC}^T L_{EC} - K_{SH}^T L_{SH} = 0. \quad (5)$$

Note that fulfilling the condition for temperature compensation does not compromise the sensor response to pressure. This is because the signs of sensitivities in the sensing and compensating elements are the same for temperature and opposite for pressure. Therefore, for the temperature compensated sensor, phase shifts induced by pressure in the sensing and compensating fiber add to each other and in consequence enhance the sensor response to pressure.

If the condition (5) is satisfied, the sensor performance versus temperature is only limited by second-order effects [11], [12], representing dependence of fiber temperature sensitivity upon pressure. It was experimentally shown in [11], [12] that in HB fibers, the parameter $\partial^2\Delta n/\partial T\partial p$ is nonzero and causes residual temperature drift in fiber-optic pressure sensors with standard temperature compensation of the order of 1% of FS per 50 °C. As in the proposed sensor configuration, pressure has access to both the sensing and the compensating element; residual temperature drift caused by second-order effects is significantly lower than in sensors with standard temperature compensation. In our case, second-order effects influence only the overall sensor response to pressure, which will change with temperature with the rate 1% per 50 °C.

The phase changes induced by pressure are detected in the decoding interferometer, which is composed of the quartz retardation plate and the analyzer aligned at an angle of 45° to the polarization axes of the plate. The plate is composed of two wedges, which can be moved with respect to each other. In this way, the thickness of the plate can be tuned. The sensor and the

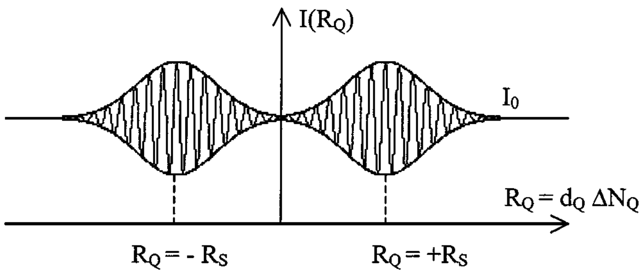

Fig. 3. Intensity variation at the sensor output as a function of group retardation of the quartz plate $R_Q = \Delta N_Q d$ and the unambiguous operation range.

decoding interferometer are connected with HB fiber (Corning PMF-38) aligned at the output at a 45° angle to the polarization axes of the quartz plate. Such alignment assures maximum contrast of the interference fringes equal to 0.5. The intensity at the output of the decoding interferometer can be expressed by the following formula:

$$I_M = I_0[1 + 0.5\gamma(R_S \pm R_Q)\sin(\Delta\phi_S \pm \Delta\phi_Q)] \quad (6)$$

where

- I_0 average light intensity at the system output;
- γ coherence function of the light source;
- R_S and R_Q total group imbalance introduced, respectively, by the sensor and the retardation plate.

Intensity variation as a function of group retardation of the quartz plate is shown in Fig. 3.

The interference signal can be observed at the output of the decoding interferometer, if the group delay ΔR_S introduced by the sensor and the group delay ΔR_Q introduced by the quartz plate match each other

$$\Delta N_{SH} L_{SH} - \Delta N_{EC} L_{EC} \pm \Delta N_Q d_Q < \tau_C \quad (7)$$

where ΔN_{SH}, ΔN_{EC}, and ΔN_Q are the group refraction indexes of the side-hole fiber, elliptical core fiber, and crystalline quartz plate, respectively; d_Q is the thickness of the quartz plate; and τ_C is a coherence length of the source. The highest contrast of interference signal is obtained when the sum of group retardations introduced by the sensor and the decoding interferometer is equal to zero. The lengths of the sensing L_{SH} and the compensating L_{EC} fibers must simultaneously satisfy conditions (1) and (3).

By moving one of the wedges constituting the quartz plate, we can tune the initial phase shift $\Delta\phi_0$ until the system operates in the most linear part of the sinusoidal characteristic, as in Fig. 3. In order to preserve an unambiguous measurement range, the phase shift induced by pressure must be lower than $\pm\pi/2$. Additionally, there is a reference photodiode in the detection system that is used to normalize the interference signal and to make it insensitive to intensity fluctuations of the light source. The optical interference signal is converted to an electronic signal by a pin-photodiode. Signals from the two photodiodes are amplified and registered by a computer. The computer board we use allows for signal registration with a sampling rate up to 10 kHz.

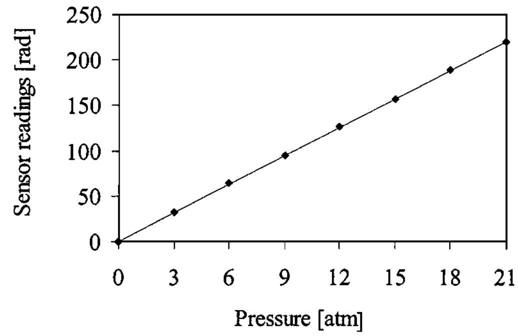

Fig. 4. Calibration of the pressure sensor, pressure sensitivity $S_P = 10.4$ rad/atm.

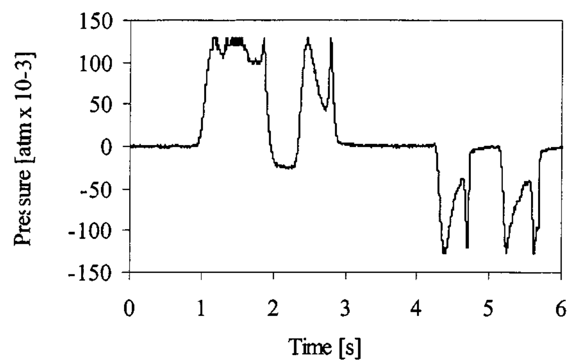

Fig. 5. Sensor response to positive and negative pressure changes exceeding the operation range.

IV. Calibration Procedure and Applications

In the first step of the calibration procedure, we measured the pressure sensitivity of the sensor. This was accomplished by applying pressure much higher than the sensor's unambiguous operation range and counting interference fringes observed in the measurement channel. By fitting the pressure characteristic of the sensor with a linear function, we determined its sensitivity to pressure: $S_P = 10.4$ rad/atm. The pressure characteristic of the sensor is shown in Fig. 4.

In the second step of the calibration procedure, we determined maximum ($I_N^{\max} = I_M^{\max}/I_{ref}$) and minimum ($I_N^{\min} = I_M^{\min}/I_{ref}$) values of the normalized intensity corresponding to pressure-induced phase shifts of $+\pi/2$ and $-\pi/2$, respectively. In order to do this, we first tuned the normalized intensity to the average value (I_N^0) at atmospheric pressure by changing the thickness of the retardation plate. To determine $I_N^{\min}$ and $I_N^{\max}$, we induced positive and negative phase increases, with respect to the atmospheric pressure, by applying respectively positive and negative pressure to the active part of the sensor. If the calibration constants $I_N^{\max}$, $I_N^{\min}$, I_N^0, and S_P are known, the pressure changes Δp can be calculated according to

$$\Delta p = \frac{1}{S_P} \arcsin \frac{2\left[I_N(\Delta p) - I_N^0\right]}{I_N^{\max} - I_N^{\min}}. \quad (8)$$

In Fig. 5, we demonstrate the sensor responses to pressure changes inducing the phase shifts higher than $\pm\pi/2$. This figure shows that unambiguous operation range of the sensor is ± 0.1 atm. We also determined the minimum detectable

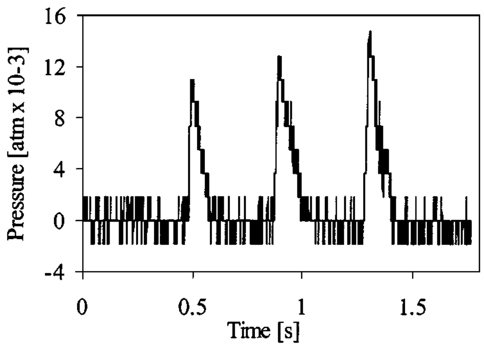

Fig. 6. Determining the minimum detectable pressure change equal to $2 \cdot 10^{-3}$ atm.

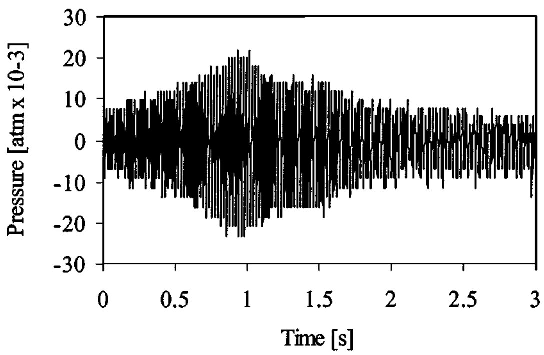

Fig. 7. Pressure changes induced by fumes in a car exhaust pipe. Negative values indicate pressure lower than atmospheric pressure.

pressure change (2×10^{-3} atm) that is associated with the noise level in the detection system (see Fig. 6).

The sensor was preliminarily tested in measurements of pressure changes induced by fumes in a car exhaust-pipe. The results are presented in Fig. 7. It is expected that simultaneous measurements of pressure and temperature changes in the exhaust-pipes of large vehicles like ships and locomotives will allow for on-line determination of the total mass of fumes released to the atmosphere.

V. Summary

The presented sensor shows remarkably high resolution of pressure measurements equal to 2×10^{-3} atm. This is the highest resolution ever reported for a pressure sensor based on HB fiber. It was possible to achieve through the application of the specially developed side-hole fiber, which is extremely sensitive to hydrostatic pressure. Another advantage of the proposed sensor is associated with the use of low coherence interferometric configuration. It reduces the noise level because the light scattered or reflected by the optical elements cannot interfere at the system output due to lack of coherence. Furthermore, it simplifies the initial tuning of the system to the most linear part of the characteristics.

The sensor measurement range can be modified by changing the lengths of the sensing and compensating fibers. Furthermore, the low-coherence intereferometric sensors can be easily multiplexed using the coherency addressing principle. To assure simultaneous readout of several sensors, their group retardations have to be significantly different, and more detection channels with retardation plates matching respective sensors have to be used in a decoding interferometer.

References

[1] J. Dakin and B. Culshaw, *Optical Fiber Sensors: Principles and Components*. Norwood, MA: Artech House, 1988, vol. 1 and 2.

[2] E. Udd, *Fiber Optic Sensors*. London, U.K.: Wiley Interscience, 1993.

[3] K. T. V. Grattan and B. T. Meggitt, *Optical Fiber Sensor Technology*. London, U.K.: Chapman & Hall, 1995.

[4] W. J. Bock and W. Urbańczyk, "Apparatus for measuring an ambient isotropic parameter applied to a highly birefringent sensing fiber using interference pattern detection," U.S. Patent 5 517 022, May 14, 1996.

[5] ——, "Temperature-desensitization of fiber-optic pressure sensor by simultaneous measurement of pressure and temperature," *Appl. Opt.*, vol. 37, pp. 3897–3901, 1998.

[6] W. J. Bock, W. Urbańczyk, and M. B. Zaremba, "Electronically scanned white-light interferometric sensor employing highly birefringent fiber," *Opt. Commun.*, vol. 101, pp. 157–162, 1993.

[7] N. Fürstenau, M. Schmidt, W. J. Bock, and W. Urbańczyk, "Dynamic pressure sensing with a fiber-optic polarimetric pressure transducer with two wavelength passive quadrature readout," *Appl. Opt.*, vol. 37, pp. 663–671, 1998.

[8] J. Wojcik, P. Mergo, W. Urbańczyk, and W. J. Bock, "Possibilities of application of the side-hole circular core fiber in monitoring of high pressures," *IEEE Trans. Instrum. Meas.*, vol. 47, pp. 805–808, Oct. 1998.

[9] W. J. Bock, W. Urbańczyk, and J. Wójcik, "Characterization of elliptical-core side-hole fiber for interferometric pressure sensing," *Proc. SPIE Interferometry*, vol. 2341, pp. 152–159, 1994.

[10] W. J. Bock, W. Urbańczyk, and M. Fontaine, "Characterization of highly birefringent optical fibers using interferometric techniques," *IEEE Trans. Instrum. Meas.*, vol. 46, pp. 903–907, Oct. 1997.

[11] W. J. Bock, W. Urbańczyk, R. Buczyński, and A. W. Domański, "Cross-sensitivity effect in temperature compensated sensors based on highly birefringent fibers," *Appl. Opt.*, vol. 33, pp. 6078–6083, 1994.

[12] W. J. Bock and W. Urbańczyk, "Temperature-hydrostatic pressure cross-sensitivity effect in elliptical core highly birefringent fibers," *Appl. Opt.*, vol. 35, pp. 6267–6270, 1996.

Wojtek J. Bock (M'85–SM'90) was born in Warsaw, Poland, in 1948. He received the M.Sc. degree in electrical engineering, with specialization in solid-state electronics, from the Faculty of Electrical Engineering at Warsaw University of Technology in 1971, and the Ph.D. degree in solid-state physics from the Institute of Physics of the same university.

For several years, he was with the Warsaw University of Technology as an Assistant Professor and also as a Head of the Laboratory of Pressure Measurements and Calibration. Since 1985, he has been with the the University of Quebec at Hull (UQAH), PQ, Canada, where he is presently a Full Professor of electrical engineering, Head of the Laboratory of Industrial Optoelectronics and Chairman of the Department of Information Technology. At UQAH, he established a successful research program in fiber-optic sensing devices and systems. He leads several large research projects aimed at practical implementation of fiber-optic sensors for the structural monitoring, including measurements of stress, load, pressure, and strain in large civil engineering and aerospace structures. He has authored and coauthored more than 200 scientific publications and holds five U.S. patents.

Dr. Bock became an active Member of the IEEE's Instrumentation and Measurement Society in 1987. As a member of its Editorial Review Board, he served many years as a frequent reviewer of the IEEE Transactions on Instrumentation and Measurement. Since 1997, he became an Associate Editor for the Transactions on Instrumentation and Measurement and since 1998, he has been serving his first term as an AdCom member. In May 1997, he was a General Chairman of the 14th Annual Instrumentation and Measurement Technology Conference in Ottawa and contributed to the success of this meeting.

Magdalena S. Nawrocka, photograph and biography not available at the time of publication.

Waclaw Urbanczyk, photograph and biography not available at the time of publication.